Applied Mathematics and Computation 356 (2019) 157–172

Contents lists available at ScienceDirect

Applied Mathematics and Computation

journal homepage: www.elsevier.com/locate/amc

A numerical scheme for solving a class of logarithmic integral equations arisen from two-dimensional Helmholtz equations using local thin plate splines

Pouria Assari[a,*], Fatemeh Asadi-Mehregan[a], Salvatore Cuomo[b]

[a] Department of Mathematics, Faculty of Sciences, Bu-Ali Sina University, Hamedan 65178, Iran
[b] Department of Mathematics and Applications, University of Naples Federico II, Naples, Italy

ARTICLE INFO

MSC:
41A25
45B05
45E10
35J05

Keywords:
Helmholtz equation
Logarithmic integral equation
Discrete collocation method
Local thin plate spline
Meshless method
Error analysis

ABSTRACT

This paper presents a numerical method for solving logarithmic Fredholm integral equations which occur as a reformulation of two-dimensional Helmholtz equations over the unit circle with the Robin boundary conditions. The method approximates the solution utilizing the discrete collocation method based on the locally supported thin plate splines as a type of free shape parameter radial basis functions. The local thin plate splines establish an efficient and stable technique to estimate an unknown function by a small set of nodes instead of all points over the solution domain. To compute logarithm-like singular integrals appeared in the method, we use a particular nonuniform Gauss–Legendre quadrature rule. Since the scheme does not require any mesh generations on the domain, it can be identified as a meshless method. The error estimate of the proposed method is presented. Numerical results are included to show the validity and efficiency of the new technique. These results also confirm that the proposed method uses much less computer memory in comparison with the method established on the globally supported thin plate splines. Moreover, it seems that the algorithm of the presented approach is attractive and easy to implement on computers.

1. Introduction

Consider the following two-dimensional Helmholtz equation

$$\Delta u(\mathbf{x}) + \lambda^2 u(\mathbf{x}) = 0, \quad \mathbf{x} \in D \subset \mathbb{R}^2, \tag{1}$$

with the Robin boundary condition

$$\frac{\partial u}{\partial n_{\mathbf{x}}} + p(\mathbf{x})u(\mathbf{x}) = g(\mathbf{x}), \quad \mathbf{x} \in \partial D,$$

where the region D is open, bounded and simply connected in $\mathbb{R}^2$ and its boundary is denoted by ∂D, $n_{\mathbf{x}}$ denotes the outward unit normal vector on ∂D, $p(\mathbf{x})$ and $g(\mathbf{x})$ are given functions on ∂D with $p(\mathbf{x}) \geq 0$ but $p \not\equiv 0$, λ is a positive wave number and the unknown function $u(\mathbf{x}) \in C^1(\bar{D}) \cap C^2(D)$ must be determined. The Helmholtz equations arise from time-harmonic

* Corresponding author.
E-mail addresses: passari@basu.ac.ir (P. Assari), f.asadi@sci.basu.ac.ir (F. Asadi-Mehregan), salvatore.cuomo@unina.it (S. Cuomo).

https://doi.org/10.1016/j.amc.2019.03.042
0096-3003/

wave propagation, and the solutions are frequently required in many applications such as aero-acoustic, underwater acoustics, electromagnetic wave scattering and geophysical problems and a large number of papers have presented many numerical methods for solving these equations [9,16,22,36,61]. It can be shown that the Helmholtz equation is uniquely solvable if λ is not an eigenvalue for the corresponding problem. It is necessary to develop a method which is uniquely solvable for all frequencies λ [40].

Integral equations have been widely applied in connection with solving boundary value problems for elliptic partial differential equations [8]. Using Green's formula, these types of partial differential equations considered on a region in $\mathbb{R}^2$ can be reformulated to equivalent integral equations over the boundary of the domain which are often called boundary integral equations. Afterward, by parameterizing this boundary, two-dimensional partial differential equations are reduced to one-dimensional Fredholm integral equations [8]. It is an attractive work to solve partial differential equations which is known in the literature as the boundary integral equation (BIE) method [6,42,44]. We use the representation

$$\mathbf{r}(t) = (\cos t, \sin t), \quad -\pi \le t \le \pi,$$

for the unit circle and, by straightforward calculations based on the Greens formula, the Helmholtz Eq. (1) can be characterized by the second-kind Fredholm integral equations with logarithmic kernels [40]

$$u(t) - \frac{1}{\pi}\int_{-\pi}^{\pi} K(t,s)u(s)\mathrm{d}s = f(t), \quad -\pi \le t, s \le \pi, \tag{2}$$

where the right-hand side function $f(t)$ is given and the kernel function $K(t, s)$ takes the form

$$K(t,s) = \ln\left|2\sin\frac{t-s}{2}\right|\left\{a_0 + a(t,s)\sin^2\frac{t-s}{2}\right\} + b(t,s),$$

in which a_0 is a constant, $a(t, s)$ and $b(t, s)$ are continuous functions of (t, s) and 2π periodic in each variable. It should be noted that we assume $u(t) \equiv u(\mathbf{r}(t))$ for simplicity in notations.

Solving analytically logarithmic integral equations are mostly difficult so, it is significant to obtain their numerical solutions. The collocation and Galerkin methods are the commonly used approaches for the numerical solutions of these integral equations. The discrete Petrov–Galerkin methods [14], piecewise polynomial collocation and Galerkin methods [53], Sinc-collocation methods [52], hybrid collocation methods [12], high-order collocation methods [24], iterated fast multiscale Galerkin methods [46], Bubnov-Galerkin methods [32], Galerkin-wavelet methods [1,25] and arbitrary collocation points (ACP) methods [15] have been applied to solve weakly singular Fredholm integral equations of the second kind. The meshless product integration (MPI) method [5] has been proposed to solve one-dimensional linear weakly singular integral equations. The Nystrom method has been used to solve weakly singular Fredholm integral equations [8,10]. Also, Khuri and Wazwaz have investigated Adomian decomposition methods for solving logarithmic Fredholm integral equations [38,66]. The methods proposed in these papers usually require some quadrature formulae to estimate the singular integrals appeared in these schemes, such as Gauss-type quadrature rules [25,37] and logarithmical Gaussian quadrature schemes [45].

The radial basis functions (RBFs) have significant applications in different problems of computational mathematics [17,18]. The selection of a parameter in most RBFs, called as the shape parameter, influences heavily on the accuracy and stability of the method. The optimal value for the shape parameters is still under the study and many authors have been suggested some alternative schemes, such as the hybrid and binary shape parameter strategies [31], the local optimization algorithm [54], cross-validation techniques [13,56] and the local Taylor expansions [33,34]. Therefore the application of free shape parameter RBFs such as the thin plate splines (TPSs) is very effective for approximating unknown functions [27,30]. Since the classical TPSs are global functions, the resultant coefficient matrix will be full and ill-condition when many points in the domain are considered to achieve high-order accurate results [11,48,64]. To overcome this problem, we can use the advantages of locally supported TPSs named as local thin plate splines (LTPSs) based on the main idea in the manuscript [41] for the local multiquadric scheme. In constructing the approximation function by LTPSs at a simple point x in the computational domain, the only geometrical data needed is the local configuration of nodes fallen within a subset of the domain which is called the influence domain corresponding to x. A valuable advantage of LTPS approximation is that its computational cost is modest in comparison with the global types and the matrix operations require only inversion of matrices of small size which is equal to the number of nodes inside the influence domain [41,55].

A large number of papers has presented numerical methods for solving several types of partial differential equations via locally supported RBFs, such as diffusion-convection problems with phase change [63], natural convection problems [39], turbulent combined forced and natural convection problems [62], natural convection under the influence of static magnetic field [50], free surface problems [35], hyperbolic PDEs [60,65], coupled Burgers' equations [59], multi-dimensional convection-dominated problems [70], 2D incompressible Navier–Stokes equations [57], diffusion equation with Dirichlet jump boundary condition [69], large-scale scattered data interpolation problems [68], the system of second-order boundary value problems [21], polarized radiative transfer in participating media [58], thermoelasticity in two dimensions [47], multi-dimensional Cahn–Hilliard, Swift–Hohenberg and phase field crystal equations [19] and simulate conservation laws equations [20].

We would like to survey some recent numerical methods for solving integral equations utilizing meshless approximations. The RBFs have been applied for solving Fredholm integral equations on non-rectangular domains with sufficiently smooth kernels [2] and weakly singular kernels [6]. The meshless product integration (MPI) method [5] has been proposed

to solve linear weakly singular integral equations. The moving least squares (MLS) collocation method has been used for solving linear and nonlinear two-dimensional integral equations on non-rectangular domains [4,49] and integro-differential equations [23]. A local meshless Galerkin method [3] has been utilized to solve weakly singular linear integral equations of the second kind. An MLS-based scheme [42,44] has been applied to the numerical solution of singular boundary integral equations [7,43]. Authors of [28,29] have investigated a domain–type RBF collocation method and a boundary–type RBF collocation method to solve some integro–differential models.

The main purpose of this paper is to provide a computational method for solving the logarithmic integral Eq. (2). These types of integral equations result from boundary value problems of Helmholtz equations over the unit circle with the Robin boundary conditions. The general framework of the current scheme is based on the collocation method together with LTPSs constructed on scattered points to estimate the unknown function. The proposed scheme uses a special accurate quadrature formula based on the nonuniform Gauss–Legendre integration rule on the local influence domain to compute logarithm-like integrals appeared in the scheme. The new technique does not require any domain elements over the solution region, so it is meshless. Moreover, we obtain the error bound and the convergence rate of the proposed approach. The presented scheme developed in the current paper is simple, computationally attractive and more flexible for most classes of logarithmic integral equations. The technique obtains more accurate results using much fewer volume computing in compared with global TPSs. The precision and convergence of the new approach are tested in various logarithmic integral equations.

The outline of the paper is as follows. In Section 2, we review some basic formulations and properties of the LTPSs method. In Sections 3, we present a computational method for solving the logarithmic integral Eq. (2) by the LTPS scheme and provide the error analysis for the proposed method. Numerical examples are given in Section 5. Finally, we conclude the article in Section 6.

2. Local thin plate spline

The one-dimensional TPS $\phi : \mathbb{R} \to \mathbb{R}$ of order $k \in \mathbb{N}$ is represented as follows [67]:

$$\phi(x) = (-1)^{k+1}|x|^{2k}\log|x|.$$

The TPSs of order k are strictly conditionally positive definite functions of degree $k+1$ on $\mathbb{R}$ [67].

We estimate a function $u(x)$ by the TPS $\phi(x)$ of order k based on the use of distinct points $\{x_1, \ldots, x_N\}$ in the interval $[a, b]$ as follows [26,67]:

$$u(x) \approx \mathcal{P}_N u(x) = \sum_{i=1}^{N} c_i \phi(x - x_i) + \sum_{\ell=0}^{k} d_\ell \mathcal{L}_\ell(x), \qquad a \le x \le b, \tag{3}$$

where $\mathcal{L}_\ell(x),\ \ell = 0, 1, \ldots, k,$ are the well-known Legendre polynomials of the degree ℓ on $[a, b]$.

The coefficients in the expansion (3) are given by the interpolation conditions

$$\mathcal{P}_N u(x_i) = u(x_i) = u_i, \qquad i = 1, \ldots, N,$$

which results a system of N linear equations in the $N + k + 1$ unknowns c_i and d_l, so we consider the following $k+1$ additional conditions to guarantee a unique solution [26]:

$$\sum_{i=1}^{N} c_i \mathcal{L}_\ell(x_i) = 0, \qquad \ell = 0, 1, \ldots, k.$$

We are ready to study the well-posedness of the interpolation problem via TPSs in the following theorem which is retrieved from a general theorem for strictly conditionally positive definite functions on the domain $D \subset \mathbb{R}^d,\ d \in \mathbb{N}$ [67].

Theorem 2.1 [67]. *Let ϕ be a TPS of order k and the set $\{x_1, \ldots, x_N\}$ give the scattered distinct points on the interval $[a, b]$, then the interpolation problem via TPSs is uniquely solvable.*

To analyze the stability of the TPS method, we require to present a definition from Wendland [67].

Definition 2.1 [26]. The separation distance of $X = \{x_1, \ldots, x_N\}$ is given by

$$q_X = \frac{1}{2}\min_{i \ne j}|x_i - x_j|.$$

To measure the stability, we define ℓ_2-condition number for the coefficient matrix A corresponding to the thin plate splines ϕ of order k and the data sites $X = \{x_1, \ldots, x_N\} \subset [a, b]$ as follows

$$\mathrm{cond}(A) = \frac{\lambda_{\max}}{\lambda_{\min}},$$

where $\lambda_{\max}$ and $\lambda_{\min}$ denote the largest and smallest eigenvalues of A [67]. First, use of Gershgorin's theorem yields during the time that the data are not too savagely distributed, the increasing $\lambda_{\max}$ will be satisfactory [67]. Therefore, the lower

bounds for $\lambda_{\min}$ must be found which eventually provides a bound for the condition number of A. The authors of [51] have established lower bounds for $\lambda_{\min}$ as follows:

$$\lambda_{\min} \geq C_d c_k (2M_d)^{-d-2k} q_X^{2k},$$

where c_k, M_d and C_d are explicit constants. It should be noted that the condition number of the global TPSs grows when the number of nodal points N increases in the domain to obtain accurate results.

Suppose $[a_i, b_i] = [x_i - r_i, x_i + r_i]$ in which $r_i > 0$ is chosen such that the set of them establishes an open bounded cover for $[a, b]$, i.e.

$$[a, b] \subseteq \bigcup_{i=1}^{N} [a_i, b_i].$$

Adopting a single cover-size r_i for all points may lead to various extreme cases. In fact, a too small value of r_i often leads to a cover having too few nodes fallen inside. Vice versa, there may be too many nodes fallen within a nodal cover in the densely populated zone when r_i is too big. In addition, a cover embracing too many nodes will definitely increase the bandwidth of the resulting matrix regardless of the nodal numbering sequence and hence pushes up the computational cost. To avoid the occurrence of these extreme scenarios, a strategy of assigning variable cover sizes to different nodes is adopted whenever non-uniform distribution of nodes is encountered [41]. The cover size r_i of the node x_i is determined as follows [41]:

1. Consider the four nearest the nodes x_j, $j = 1, 2, 3, 4$ to x_i.
2. Define
$$d_i = \max_{j=1,2,3,4} |x_i - x_j|.$$
3. Determine the cover size r_i of x_i such that $r_i = \rho d_i$, where ρ is a constant > 1.

We can estimate the function $u(x)$ on $[a_i, b_i]$, $i = 1, \ldots, N$, as follows:

$$u(x) \approx \mathcal{R}_i u(x) = \sum_{j \in I_i} c_j^i \phi^i(x - x_j) + \sum_{\ell=0}^{k} d_\ell^i \mathcal{L}_\ell^i(x), \quad x \in [a_i, b_i], \tag{4}$$

where I_i is the set of indexes corresponding to points fallen within the influence domain $[a_i, b_i]$ (or cover) with the cardinal number $|I_i| = n_i$.

To ensure the unique solution for the problem (4), we need to enforce n_i interpolation conditions

$$\mathcal{R}_i u(x_r) = u_r, \quad r \in I_i, \tag{5}$$

and $k + 1$ additional equations

$$\sum_{j \in I_i} c_j^i \mathcal{L}_\ell^i(x_j) = 0, \quad \ell = 0, 1, \ldots, k. \tag{6}$$

Similar to the idea presented in the manuscript [41], we can obtain $c_{k'_\ell}^i$, $\ell = 0, \ldots, k$ from the system (6) as follows:

$$c_{k'_\ell}^i = \sum_{j \in I_i, j \neq k'_0, \ldots, k'_k} \alpha_j^{k'_\ell} c_j^i, \quad \ell = 0, \ldots, k,$$

where

$$\alpha_j^{k'_\ell} = -\frac{1}{\mathcal{L}_\ell^i(x_{k'_\ell})} \left(\sum_{\nu=0}^{\ell-1} c_{k'_\nu}^i \mathcal{L}_\ell^i(x_{k'_\nu}) + \mathcal{L}_\ell^i(x_j) - \sum_{\nu=\ell+1}^{k} \frac{\mathcal{L}_\nu^i(x_j)}{\mathcal{L}_\nu^i(x_{k'_\nu})} \right), \quad \ell = 0, \ldots, k. \tag{7}$$

Therefore, the expansion (4) can be rewritten as

$$\mathcal{R}_i u(x) = \sum_{j \in I_i, j \neq k'_0, \ldots, k'_k} c_j^i g_j^i(x) + \sum_{\ell=0}^{k} d_\ell^i \mathcal{L}_\ell^i(x), \quad x \in [a_i, b_i], \tag{8}$$

where

$$g_j^i(x) = \phi^i(x - x_j) + \sum_{\ell=0}^{k} \alpha_j^{k'_\ell} \phi^i(x - x_{k'_\ell}).$$

From (7), we conclude that the additional coefficients $d_\ell^i, \ell = 0, \ldots, k$ can be replaced by $c_{k'_\ell}, \ell = 0, \ldots, k$ [41]. Thus, the expansion (8) can be reformulated as

$$\mathcal{R}_i u(x) = \sum_{j \in I_i} c_j^i g_j^i(x).$$

On the other hand, we consider the following matrix form for the linear system (5) as:

$$\mathbf{B}^i\mathbf{C}^i = \mathbf{U}^i,$$

where

$$\mathbf{U}^i = [u_1, u_2, \ldots, u_{n_i}]^T, \quad \mathbf{C}^i = [c_1, c_2, \ldots, c_{n_i}]^T,$$

and $\mathbf{B}^i = [g_j(x_r)]_{n_i \times n_i}$ is a real symmetric coefficient matrix. If we define

$$\varphi^i(x) = [g_1(x), g_2(x), \ldots, g_{n_i}(x)]^T, \tag{9}$$

then the expansion $\mathcal{R}_i u(x)$ and the matrix $\mathbf{B}^i$ can be expressed as

$$\mathcal{R}_i u(x) = \varphi^i(x)^T \mathbf{C}^i.$$

From Theorem 2.1, we know that the matrix $\mathbf{B}^i$ is invertible and so the vector $\mathbf{C}^i$ is obtained by

$$\mathbf{C}^i = (\mathbf{B}^i)^{-1}\mathbf{U}^i.$$

Therefore, it results that [41]

$$\mathcal{R}_i u(x) = \varphi^i(x)^T (\mathbf{B}^i)^{-1}\mathbf{U}^i = \Psi^i(x)^T \mathbf{U}^i,$$

or equivalently

$$\mathcal{R}_i u(x) = \sum_{j \in I_i} u_j \psi_j^i(x),$$

where

$$\psi_j^i(x) = \sum_{k \in I_i} [(\mathbf{B}^i)^{-1}]_{kj} g_k^i(x), \quad j \in I_i.$$

It can be easily proved that the support of $\psi_j^i(x)$ is the interval $[a_i, b_i]$ and satisfies the Kronecker delta condition [41], .i.e.

$$\psi_j^i(x_i) = \delta_{ij}, \quad i, j \in I_i, \tag{10}$$

We explain the LTPS collocation method to approximate a function $u(x)$ at an arbitrary point $x \in [a, b]$ as follows:

$$u(x) \approx \mathcal{G}_N u(x) = \sum_{i=1}^{N} u_i \psi_i^i(x), \quad x \in [a, b], \tag{11}$$

where the functions $\psi_i^i(x)$ are called as the shape functions of the LTPS interpolation.

Since many terms in the expansion (11) will vanish, we can assume that

$$\mathcal{G}_N u(x) = \sum_{i \in I_x} u_i \psi_i^i(x), \quad x \in [a, b],$$

where $I_x = \{i : x \in [a_i, b_i]\}$ and the influence domain of the point x is $D_x = \cup_{i \in I_x}[a_i, b_i]$.

3. Solution of logarithmic integral equations

Let $\mathcal{K} : C([-\pi, \pi]) \to C([-\pi, \pi])$ be the logarithmic singular integral operator as follows:

$$\mathcal{K}u(t) = \int_{-\pi}^{\pi} \left[\ln \left| 2 \sin \frac{t-s}{2} \right| \left\{ a_0 + a(t,s) \sin^2 \frac{t-s}{2} \right\} + b(t,s) \right] u(s) \mathrm{d}s. \tag{12}$$

The integral operator $\mathcal{K}$ with the logarithmic kernel is a compact operator on $C([-\pi, \pi])$ [40].

Utilizing the operator (12), we can rewrite the integral Eq. (2) as

$$(I - \frac{1}{\pi}\mathcal{K})u = f.$$

To apply the LTPS method for solving the integral Eq. (2), we require N nodal points in the interval $[-\pi, \pi]$. The distribution of these nodes could be selected regularly or randomly as

$$-\pi \le t_1 < \cdots < t_N \le \pi.$$

Therefore the unknown function $u(x)$ can be approximated by the LTPSs as

$$u(t) \approx \sum_{i=1}^{N} c_i \psi_i^i(t), \quad -\pi \le t \le \pi. \tag{13}$$

By replacing the expansion (13) with $u(t)$ and pick distinct node points $t_1, t_2, \ldots, t_N \in [-\pi, \pi]$ in the integral Eq. (2), we obtain

$$\sum_{i=1}^{N} c_i \left(\psi_i^i(t_j) - \frac{1}{\pi} \int_{-\pi}^{\pi} K(t_j, s) \psi_i^i(s) \mathrm{d}s \right) = f(t_j), \quad j = 1, \ldots, N,$$

where

$$K(t_j, s) = \ln \left| 2 \sin \frac{t_j - s}{2} \right| \left\{ a_0 + a(t_j, s) \sin^2 \frac{t_j - s}{2} \right\} + b(t_j, s).$$

Since the support of the shape functions $\psi_i^i(t)$ is $[\alpha_i, \beta_i] = [t_i - r_i, t_i + r_i]$ and also the shape functions $\psi_i^i(t)$ satisfy the Kronecker delta condition from (10), it leads to

$$c_j - \frac{1}{\pi} \sum_{i=1}^{N} c_i \int_{\alpha_i}^{\beta_i} K(t_j, s) \psi_i^i(s) \mathrm{d}s = f(t_j), \quad j = 1, \ldots, N, \tag{14}$$

where

$$\alpha_i = \max\{-\pi, t_i - r_i\}, \quad \text{and} \quad \beta_i = \min\{\pi, t_i + r_i\}.$$

The discrete collocation method results from the numerical integration of all integrals in the system (14) associated with the collocation method [8]. Therefore, there are two types of integrals to be evaluated as

$$I_{ij} = \underbrace{\int_{\alpha_i}^{\beta_i} \ln \left| 2 \sin \frac{t_j - s}{2} \right| \left\{ a_0 + a(t_j, s) \sin^2 \frac{t_j - s}{2} \right\} \psi_i^i(s) \mathrm{d}s}_{I_{ij,1}} + \underbrace{\int_{\alpha_i}^{\beta_i} b(t_j, s) \psi_i^i(s) \mathrm{d}s}_{I_{ij,2}}.$$

Since the right-hand side integral $I_{ij,1}$ is singular at the point t_j, this integral appeared in the scheme cannot be estimated by classical integration rules, such as commonly Gauss–Legendre quadrature rules. In the following, we present a simple but efficient quadrature rule from Fang et al. [25] for computing such integrals.

Now, we present the composite m_N-point Gauss–Legendre quadrature rule for weakly singular integrals with M non-uniform subdivisions. Let $h(s)$ be defined on $(0, 1)$ and near $s = 0$ satisfy

$$|h^{(2m_N)}(s)| \leq C s^{-r-2m_N}, \quad \text{for som } r \in (0, 1), \tag{15}$$

and for all $s \in (0, 1)$. Suppose $\{v_k\}$ are the m_N zero of the Legendre polynomial of degree m_N on $[-1, 1]$ and $\{w_k\}$ are weights for Gauss–Legendre quadrature rule. Then, for any given integer $M > 0$, we have

$$\int_0^1 h(s) \mathrm{d}s = \sum_{q=1}^{M} \sum_{k=1}^{m_N} w_k \frac{\Delta s_q}{2} f(\theta_k^q) + \mathcal{O}\left(\frac{1}{M^{2m_N}}\right), \tag{16}$$

where

$$\Delta s_q = s_q - s_{q-1}, \ \bar{s}_q = \frac{s_q + s_{q-1}}{2}, \ \theta_k^q = \frac{\Delta s_q}{2} v_k + \bar{s}_q,$$

with $s_q = \left(\frac{q}{M}\right)^p$, $p = \left(\frac{2m_N + 1}{1 - r}\right)$.

It is easy to see that the integral $I_{ij,1}$ singular along the point t_j, so the quadrature rule (16) can not be applied for this integral. Therefore, we consider the decomposition

$$\begin{aligned} I_{ij,1} = & \int_{\alpha_i}^{t_j} \ln \left| 2 \sin \frac{t_j - s}{2} \right| \left\{ a_0 + a(t_j, s) \sin^2 \frac{t_j - s}{2} \right\} \psi_i^i(s) \mathrm{d}s \\ & + \int_{t_j}^{\beta_i} \ln \left| 2 \sin \frac{t_j - s}{2} \right| \left\{ a_0 + a(t_j, s) \sin^2 \frac{t_j - s}{2} \right\} \psi_i^i(s) \mathrm{d}s. \end{aligned}$$

By the following simple change of variables

$$x = \frac{t_j - s}{\alpha_i - t_j}, \quad \text{and} \quad y = \frac{s - t_j}{\beta_i - t_j},$$

the integral $I_{ij,1}$ can be written as

$$I_{ij,1} = (t_j - \alpha_i) \int_0^1 \mathcal{H}_1[ij, x, \psi_i^i] \mathrm{d}x + (\beta_i - t_j) \int_0^1 \mathcal{H}_2[ij, y, \psi_i^i] \mathrm{d}y,$$

where

$$\mathcal{H}_1[t_j, x, \psi_i^i] = \ln\left|2\sin\frac{(t_j(\alpha_i - t_j)x)}{2}\right|\left\{a_0 + a(t_j, t_j - x(\alpha_i - t_j))\sin^2\frac{(t_j(\alpha_i - t_j)x)}{2}\right\}\psi_i^i(t_j - x(\alpha_i - t_j)),$$

and

$$\mathcal{H}_2[t_j, y, \psi_i^i] = \ln\left|2\sin\frac{(\beta_i - t_j)y}{2}\right|\left\{a_0 + a(t_j, t_j - y(\alpha_i - t_j))\sin^2\frac{(\beta_i - t_j)y}{2}\right\}\psi_i^i(t_j - y(\alpha_i - t_j)).$$

By this representation of the integral $I_{ij,1}$, the functions $\mathcal{H}_1[ij, x, \psi_i^i]$ and $\mathcal{H}_2[ij, y, \psi_i^i]$ satisfy the condition (15) for any positive integer m_N and for any small positive number r, since it has the weakly singularity in $x = 0$ and $y = 0$ [25,37]. Now, the numerical integration rule (16) can be applied in these integrals, so

$$I_{ij,1} = \sum_{q=1}^{M}\sum_{k=1}^{m_N} w_k\frac{\Delta x_q}{2}\mathcal{F}_1[t_j, \theta_k^q, \psi_i^i] + \mathcal{O}(\frac{1}{M^{2m_N}}), \tag{17}$$

where

$$\mathcal{F}_1[t_j, \theta_k^q, \psi_i^i] = (t_j - \alpha_i)\mathcal{H}_1[t_j, \theta_k^q, \psi_i^i] + (\beta_i - t_j)\mathcal{H}_2[t_j, \theta_k^q, \psi_i^i].$$

On the other hand, to approximate the integral $I_{ij,2}$, we use the composite m_N-point Gauss–Legendre rule with M uniform subdivisions relative to the coefficients $\{v_\ell\}$ and weights $\{w_\ell\}$ in the interval $[-1, 1]$ as

$$I_{ij,2} = \frac{\Delta x_i}{2}\sum_{p=1}^{M}\sum_{\ell=1}^{m_N} w_\ell b(t_j, \tau_{\ell,i}^p)\psi_i^i(\tau_{\ell,i}^p) + \mathcal{O}(\frac{1}{M^{2m_N}}), \tag{18}$$

where $\Delta x_i = \frac{\beta_i - \alpha_i}{M}$ and $\tau_{\ell,i}^p = \frac{\Delta x_i}{2}v_\ell + (p - \frac{1}{2})\Delta x_i$.

Utilizing the quadrature formulae (17) and (18), for all integrals in the system (14), the following system is obtained

$$\hat{c}_j - \frac{1}{\pi}\sum_{i=1}^{N}\hat{c}_i\left(\sum_{q=1}^{M}\sum_{k=1}^{m_N} w_k\frac{\Delta x_q}{2}\mathcal{F}_1[t_j, \bar{\theta}_k^q, \psi_i^i] + \frac{\Delta x_i}{2}\sum_{p=1}^{M}\sum_{\ell=1}^{m_N} w_\ell b(t_j, \tau_{\ell,i}^p)\psi_i^i(\tau_{\ell,i}^p)\right) = f(x_j), \tag{19}$$

A sequence of numerical integral operators $\mathcal{K}_N$, $N \geq 1$ on $C[a, b]$ is also introduced by

$$\mathcal{K}_N u(t) = \sum_{q=1}^{M}\sum_{k=1}^{m_N} w_k\frac{\Delta h_q}{2}\mathcal{F}_1[t, \theta_k^q, u] + \frac{\Delta x_i}{2}\sum_{p=1}^{M}\sum_{\ell=1}^{m_k} w_\ell b(t_j, \tau_{\ell,i}^p)u(\tau_{\ell,i}^p).$$

It should be noted that $\{\mathcal{K}_N\}$ is a collectively compact family that is pointwise convergent [25] and there is the constant $C_N > 0$ such that

$$\|\mathcal{K}u - \mathcal{K}_N u\| \leq \frac{C_N}{M^{2m_N}}\sup_{-\pi\leq t\leq\pi}|u^{(2m_N)}(t)|, \quad u \in C^{(2m_N)}[-\pi, \pi]. \tag{20}$$

We can rewrite the system (19) in the operator form as

$$(I - \frac{1}{\pi}\mathcal{G}_N\mathcal{K}_N)\hat{u}_N = \mathcal{G}_N f,$$

where the solution $\hat{u}_N$ is gotten by the proposed scheme which is obtained by solving this system for $\{\hat{c}_1, \ldots, \hat{c}_N\}$. Thus, by solving this system, the values of $u(t)$ can be evaluated by

$$\hat{u}_N(t) = \sum_{i=1}^{N}\hat{c}_i\psi_i^i(t).$$

We define the iterated discrete collocation solution by

$$\bar{u}_N = f + \frac{1}{\pi}\mathcal{G}_N\mathcal{K}_N\hat{u}_N. \tag{21}$$

Then it is easily seen that

$$\mathcal{G}_N\bar{u}_N = \hat{u}_N,$$

and consequently

$$(I - \frac{1}{\pi}\mathcal{K}_N\mathcal{G}_N)\bar{u}_N = f.$$

We give the following theorem from Atkinson [8] about the error analysis of iterated collocation method.

Theorem 3.1 [8]. *Assume that V is the framework of some complete function space on $[a, b]$ and*

A1. *$\{\mathcal{Q}_N\}$ is a family of interpolatory projection operators on V to $V_N \subset V$ and $\mathcal{Q}_N u \to u$ as $N \to \infty$ for all $u \in V$.*
A2. *$\{\mathcal{K}_N\}$ is a collectively compact family on V and pointwise convergent for all $u \in V$.*
A3. *$\bar{u}_N$ is a unique solution of the equation $(I - \lambda \mathcal{K}_N \mathcal{Q}_N)\bar{u}_N = f$, where λ is a positive constant.*

Then $(I - \lambda \mathcal{K}_N \mathcal{Q}_N)^{-1}$ exists for all sufficiently large N, say $N > \bar{M}$, and is uniformly bounded.

Now, we are ready to obtain the error estimate and the convergence rate of the new scheme based on the use of Theorem 3.1. But before that, the error estimate of LTPs interpolation is presented in terms of the fill distance parameter which is defended as follows:

Definition 3.1. For a set of points $X = \{x_1, \ldots, x_N\} \subset [a, b]$, the fill distance of X is described by

$$h_{X,[a,b]} = \sup_{a \le x \le b} \min\{|x - x_i| : i = 1, \ldots, N\}.$$

Also, we call also the set X as a quasi-uniform set corresponding to a constant $c > 0$ if

$$q_X \le h_{X,[a,b]} \le c q_X.$$

Now the error analysis of the global TPS interpolation is described which mostly follows from Wendland [67].

Theorem 3.2 [67]. *Let $u(x)$ be in the Sobolev space $W_2^{2k}(\mathbb{R})$ and the set $X = \{x_1, \ldots, x_N\} \subset [a, b]$ consist of distinct points on the interval $[a, b]$. Then there exist constants h_0, $C > 0$ such that*

$$\|u - \mathcal{P}_N u\|_\infty \le C h_{X,[a,b]}^{2k-1} \|u^{(k)}\|_{L_2[a,b]},$$

provided that $h_{X,[a,b]} \le h_0$.

As a conclusion from Theorem 3.2, there exist constants $h_{0,x}$, $C_x > 0$ such that

$$\|u - \mathcal{G}_N u\| \le C_x h_{I_x,D_x}^{2k-1} |u|_{L_2(D_x)}, \quad x \in D_x,$$

provided $h_{I_x,D_x} \le h_{0,x}$. Therefore, by considering

$$\bar{h}_{X,[a,b]} = \max_{x \in [a,b]} h_{I_x,D_x},$$

so that $h_{X,[a,b]} \le \bar{h}_{X,[a,b]}$, we have

$$\|u - \mathcal{G}_N u\| \le \bar{C} \bar{h}_{X,[a,b]}^{2k-1} \|u\|_{a,b}, \quad x \in [a, b],$$

where

$$\bar{C} = \max_{x \in [a,b]} C_x, \quad \text{and} \quad \|u\|_{a,b} = \max \|u\|_{L_2(D_x)}.$$

Let $u_0 \in W_2^{2k}[-\pi, \pi] \cap C^{2m_N}[-\pi, \pi]$ be a unique exact solution of the logarithmic integral Eq. (2). Assume the method has been installed on the quasi-uniform set X on the interval $[-\pi, \pi]$, then $\mathcal{G}_N u \to u$ as $N \to \infty$ based on the error bound (3). Theorem 3.1 find that $\bar{u}_N$ is a solution of the iterated method and there exists $\bar{M} > 0$ such that $(I - \frac{1}{\pi}\mathcal{K}_N \mathcal{G}_N)^{-1}$ exists for every $N \ge \bar{M}$ and bounded, namely

$$\|(I - \frac{1}{\pi}\mathcal{K}_N \mathcal{G}_N)^{-1}\| < \gamma_1.$$

This yields that

$$\|\bar{u}_N - u_0\|_\infty \le \gamma_1 \|\mathcal{K} u_0 - \mathcal{K}_N \mathcal{G}_N u_0\|_\infty.$$

By considering $\hat{u}_N = \mathcal{G}_N \bar{u}_N$, it results that $\hat{u}_N$ is a solution for the new scheme, because by taking $\mathcal{P}_N$ from both sides of Eq. (21), we obtain

$$\mathcal{G}_N \bar{u}_N = \mathcal{G}_N f + \frac{1}{\pi}\mathcal{G}_N \mathcal{K}_N \hat{u}_N \;\Rightarrow\; (I - \frac{1}{\pi}\mathcal{G}_N \mathcal{K}_N)\hat{u}_N = \mathcal{G}_N f.$$

The existence and boundedness of $(I - \frac{1}{\pi}\mathcal{K}_N \mathcal{G}_N)^{-1}$ eventuate forthwith the existence and boundedness of $(I - \frac{1}{\pi}\mathcal{G}_N \mathcal{K}_N)^{-1}$ [8], since

$$(I - \frac{1}{\pi}\mathcal{G}_N \mathcal{K}_N)^{-1} = \lambda\Big[I - \mathcal{G}_N (I - \frac{1}{\pi}\mathcal{K}_N \mathcal{G}_N)^{-1} \mathcal{K}_N\Big], \qquad \hat{M} \ge \bar{M} \ge N.$$

This results that $\hat{u}_N$ is a unique solution for the presented method. From the pointwise convergence of $\{\mathcal{K}_N\}$ (see [8], Theorem A.3), we can assume that $\|\mathcal{K}_N\| \le \gamma_2$. On the other hand

$$\|\hat{u}_N - u_0\|_\infty \le \gamma_1 \gamma_2 \|u_0 - \mathcal{G}_N u_0\|_\infty + \gamma_1 \|\mathcal{K} u_0 - \mathcal{K}_N u_0\|_\infty.$$

Considering $\bar{h} \equiv \bar{h}_{X,[-\pi,\pi]}$ and using (20) and (3), we obtain

$$\|\hat{u}_N - u_0\|_\infty \leq \gamma_1\gamma_2\bar{C}\bar{h}^{2k-1}\|u\|_{-\pi,\pi} + \frac{\gamma_1 C_N}{M^{2m_N}} \sup_{-\pi\leq t\leq\pi} |u_0^{(2m_N)}(t)|. \tag{22}$$

Remark 1. The error bound (22) results that the error of the scheme presented in the current paper appertains to the error of the m_N-point numerical integration method and the LTPS error. It is concluded that for sufficiently large integration nodes the error of the LTPS is dominated by the error of integration rule. Therefore increasing m_N has no important effect on the global error and the approximation order of the proposed method will be of $\mathcal{O}(\bar{h}^{2k-1})$. Moreover, utilizing weaker norms i.e., L_2-error to measure the error, we can improve the convergence order which will be of order $\mathcal{O}(\bar{h}^{2k+2})$. But the order of accuracy near the endpoints is of $\mathcal{O}(\bar{h}^{k+\frac{1}{2}})$ for general smooth data functions which this fact is effective on the global error [11].

4. Numerical examples

To test the efficiency and accuracy of the proposed method, four logarithmic Fredholm integral equations are solved. We apply LTPSs with different orders by adding fixed polynomials in the method. In illustrative examples, we put $\rho = 2$ [41]. We employ 5-points composite Gauss–Legendre quadrature rule with $M = 5$ for approximating integrals in the scheme. The error bound (22) shows that for a sufficiently large number of integration points, the error of the LTPS interpolation is dominated over the quadrature error. Therefore, increasing the number of nodes in the numerical integration method has no significant effect on the error. We also compare the results obtained in Examples 4.2 and 4.4 with the meshless discrete Galerkin (MDG) method [3]. The MDG is a technique for solving logarithmic integral equations which is based on the moving least squares by combining the Galerkin method. For the tests in the MDG method, we used the linear ($q = 1$) and quadratic ($q = 2$) basis functions and the Gaussian weight functions [3]. The following conclusions have been given in comparison with numerical results:

✓ The obtained results by the scheme presented in the current paper are better than the results given by the MDG method.

✓ The convergence rates of the proposed scheme are higher than the convergence rates of the MDG method.

✓ The CPU times of the method presented in the current paper are lower than the MDG method.

✓ Since determining the shape functions of the moving least squares requires computing an inverse matrix in each step, the algorithm of the method is simpler than the MDG method.

We have measured the accuracy of the presented technique by the maximum error $\|e_N\|_\infty$ and the mean error $\|e_N\|_2$ which can be defined as follows:

$$\|e_N\|_\infty = \max_{-\pi\leq t\leq\pi}\{|u_{ex}(t) - \hat{u}_N(t)|\}, \qquad \|e_N\|_2 = \left(\int_{-\pi}^{\pi} |u_{ex}(t) - \hat{u}_N(t)|^2 \mathrm{d}t\right)^{\frac{1}{2}},$$

where the exact solution $u_{ex}(t)$ is estimated by the numerical solution $\hat{u}_N(t)$ obtained in the current paper. The convergence rate of the presented scheme has been also reported by

$$Ratio = \frac{\ln(\|e_N\|_\infty) - \ln(\|e_{N'}\|_\infty)}{\ln(\bar{h}'_X) - \ln(\bar{h}_X)}.$$

We have written all routines in "Maple" software (with the Digits environment variable assigned to be 20) and a Laptop equipped with 2.10 GHz of Core 2 CPU and 4 GB of RAM has been used to run these. To solve the final linear system of algebraic equations the "LinearSolve" command from "Linear Algebra" package has been employed.

Example 4.1. Consider the following logarithmic integral equation:

$$u(t) - \frac{1}{\pi}\int_{-\pi}^{\pi}\left[\ln\left|2\sin\frac{t-s}{2}\right|\left\{1 + e^{ts}\sin^2\frac{t-s}{2}\right\} + \frac{1}{s^2+t^2+1}\right]u(s)\mathrm{d}s = f(t) \tag{23}$$

where the function $f(t)$ has been so chosen that the exact solution is

$$u_{ex}(x) = \cosh\left(\frac{1}{t^2+7t+1}\right).$$

The classical methods to numerically solve these types of singular integral equations have deficiencies, but this problem can be easily solved via the local meshless method presented in this work based on some random nodes on the interval $[-\pi, \pi]$. Table 1 reports $\|e\|_\infty$, $\|e\|_2$ and the values of the ratio at different numbers of N and k. We also compared the obtained errors for $k = 1, 2, 3, 4$ and different numbers of N in Fig. 1 drawn in the logarithmic mode. It is seen that the obtained numerical results converge to the exact values along with the increase of the nodes N and the convergence rates grow by increasing the order k. All results have confirmed the theoretical error estimate.

Table 1
Some numerical results for Example 4.1.

N	$k=1$		$k=2$		$k=3$	
	$\|e_N\|_2$	$\|e_N\|_\infty$	$\|e_N\|_2$	$\|e_N\|_\infty$	$\|e_N\|_2$	$\|e_N\|_\infty$
40	4.97e-03	1.38e-02	1.57e-05	4.41e-05	5.11e-08	1.43e-07
50	1.90e-03	5.36e-03	3.50e-06	9.86e-06	7.06e-09	1.94e-08
60	7.82e-04	2.18e-03	9.01e-07	2.52e-06	1.19e-09	3.25e-09
70	3.15e-04	8.67e-04	2.39e-07	6.56e-07	2.44e-10	5.93e-10
80	1.16e-04	2.99e-04	6.23e-08	1.55e-07	5.82e-11	1.23e-10
90	3.76e-05	7.96e-05	2.13e-08	4.18e-08	2.03e-11	2.45e-11

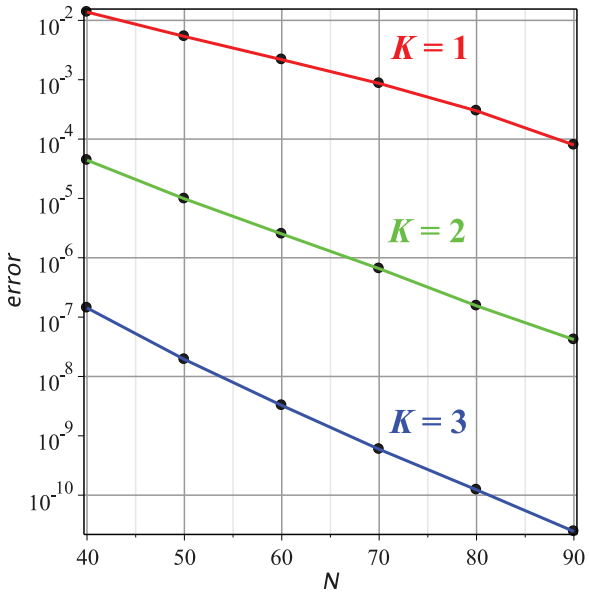

Fig. 1. Distribution of absolute error for Example 4.1.

Table 2
Some numerical results for Example 4.2.

N	$k=1$		$k=2$		$k=3$	
	$\|e_N\|_2$	$\|e_N\|_\infty$	$\|e_N\|_2$	$\|e_N\|_\infty$	$\|e_N\|_2$	$\|e_N\|_\infty$
40	6.45e-04	1.75e-03	8.50e-06	2.37e-05	1.18e-07	3.29e-07
50	1.68e-04	4.20e-04	1.19e-06	3.38e-06	1.08e-08	2.91e-08
60	4.90e-05	1.04e-04	1.97e-07	5.48e-07	1.29e-09	3.25e-09
70	1.13e-05	2.38e-05	3.28e-08	8.90e-08	2.21e-10	3.97e-10
80	2.69e-06	6.40e-06	5.04e-09	1.18e-08	4.74e-12	8.12e-11
90	5.46e-07	1.26e-06	3.83e-10	1.54e-09	9.57e-12	2.08e-11

Example 4.2. Consider the following logarithmic integral equation:

$$u(t)-\frac{1}{\pi}\int_{-\pi}^{\pi}\left[\ln\left|2\sin\frac{t-s}{2}\right|\left\{\pi+\frac{t+s}{t+s+\pi}\sin^2\frac{t-s}{2}\right\}+\cos s+t+1\right]u(s)\mathrm{d}s=f(t) \tag{24}$$

where the function $f(t)$ has been so chosen that the exact solution is

$$u_{ex}(x)=\sqrt{t^3+t+\pi}.$$

Table 2 reports $\|e\|_\infty$, $\|e\|_2$ and the values of the ratio at different numbers of N and k. We also solve the integral Eq. (24) utilizing the MDG method and the numerical results are given in Table 3. As we can see, the results gradually converge to the exact values as the number of nodes increases. The obtained errors for different numbers of N are drawn in the logarithmic mode in Fig. 2. We have compared the CPU times (sec.) for solving this integral equation using global and local TPSs and MDG for different numbers of N in Fig. 3. It is clear that the CPU times for the proposed method are much lower than the CPU times for the global RBF and MDG schemes. This comparison confirms that the new scheme is faster than the mentioned methods.

Table 3
Some numerical results for Example 4.2 using the MDG method.

N	$q=1$			$q=2$		
	δ	$\|e_N\|_2$	$\|e_N\|_\infty$	δ	$\|e_N\|_2$	$\|e_N\|_\infty$
40	0.051	1.64e-04	3.08e-04	0.077	9.62e-06	1.82e-05
50	0.041	1.05e-04	1.97e-04	0.061	4.94e-06	9.29e-06
60	0.034	7.28e-05	1.36e-04	0.051	2.89e-06	5.43e-06
70	0.029	5.44e-05	1.02e-04	0.043	1.86e-06	3.42e-06
80	0.025	4.21e-05	7.73e-05	0.038	1.26e-06	2.31e-06
90	0.022	3.34e-05	6.11e-05	0.034	8.72e-07	1.62e-06

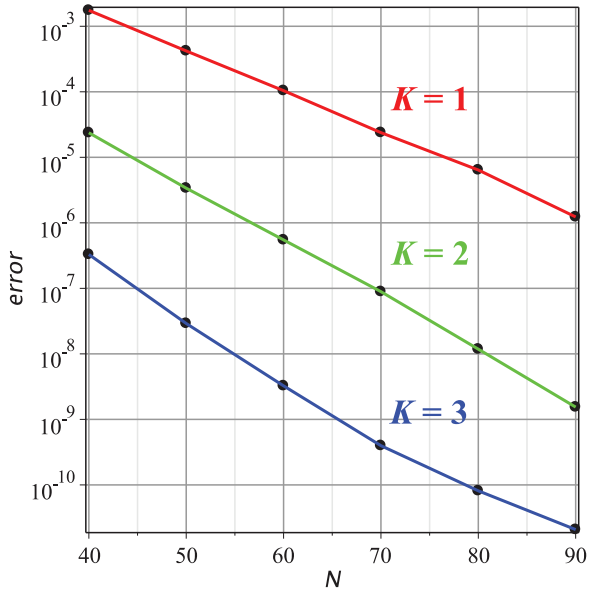

Fig. 2. Distribution of absolute error for Example 4.2.

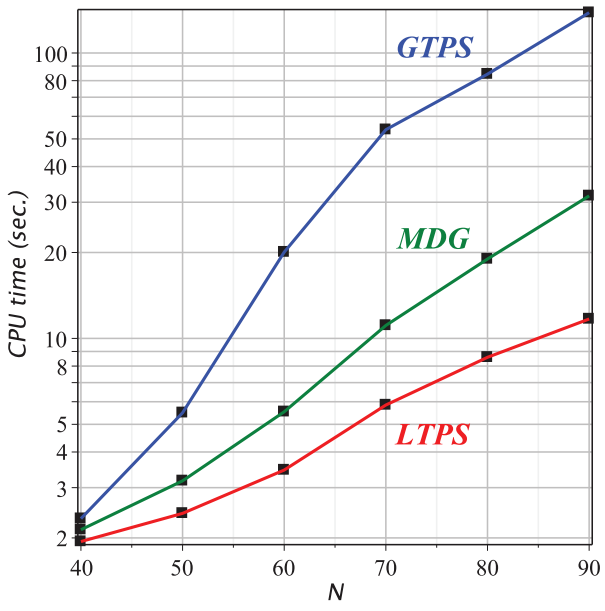

Fig. 3. CPU times for Example 4.2.

Table 4
Some numerical results for Example 4.3.

N	$k=1$		$k=2$		$k=3$	
	$\|e_N\|_2$	$\|e_N\|_\infty$	$\|e_N\|_2$	$\|e_N\|_\infty$	$\|e_N\|_2$	$\|e_N\|_\infty$
40	5.85e-02	1.62e-01	3.73e-04	1.04e-03	2.43e-06	6.82e-06
50	2.28e-02	6.43e-02	8.51e-05	2.39e-04	3.42e-07	9.51e-07
60	9.51e-03	2.65e-02	2.21e-05	6.17e-05	5.96e-08	1.61e-07
70	3.85e-03	1.06e-02	5.95e-06	1.63e-05	1.22e-08	2.99e-08
80	1.42e-03	3.70e-03	1.56e-06	3.91e-06	2.94e-09	6.16e-09
90	4.50e-04	9.52e-04	5.37e-07	1.05e-06	1.02e-09	2.25e-09

Table 5
Some numerical results for Example 4.4.

N	$k=1$		$k=2$		$k=3$	
	$\|e_N\|_2$	$\|e_N\|_\infty$	$\|e_N\|_2$	$\|e_N\|_\infty$	$\|e_N\|_2$	$\|e_N\|_\infty$
40	2.36e-02	6.57e-02	9.74e-05	2.72e-04	4.11e-07	1.15e-06
50	9.12e-03	2.56e-02	2.18e-05	6.15e-05	5.67e-08	1.57e-07
60	3.76e-03	1.05e-02	5.64e-06	1.57e-05	9.77e-09	2.65e-08
70	1.51e-03	4.18e-03	1.50e-06	4.12e-06	1.99e-09	4.85e-09
80	5.61e-04	1.45e-03	3.12e-07	9.83e-07	4.79e-10	1.01e-09
90	1.79e-04	4.21e-04	1.34e-07	2.64e-07	1.66e-10	3.65e-10

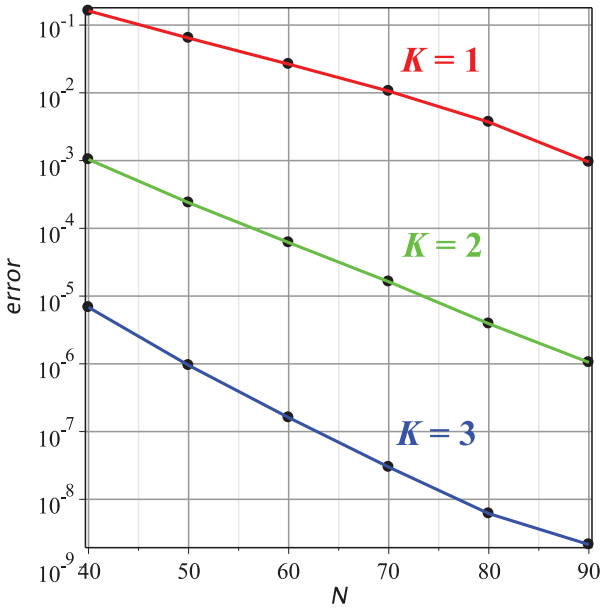

Fig. 4. Distribution of absolute error for Example 4.3.

Example 4.3. Consider the following logarithmic integral equation:

$$u(t)-\frac{1}{\pi}\int_{-\pi}^{\pi}\left[\ln\left|2\sin\frac{t-s}{2}\right|\left\{\frac{2}{3}+\sqrt{\frac{1}{t+s+3}}\sin^2\frac{t-s}{2}\right\}+\frac{7}{2}t+1\right]u(s)\mathrm{d}s=f(t) \tag{25}$$

where the function $f(t)$ has been so chosen that the exact solution is

$$u_{ex}(x)=\ln\left(2\pi+\frac{1+t}{t^2+\pi}\right).$$

Table 4 reports $\|e\|_\infty$, $\|e\|_2$ and the values of the ratio at different numbers of N and k. Apparently, the method provides accurate numerical solutions for the logarithmic integral equation. Although the error near the boundary occasionally increases which consequently effects on the maximum error, but the ratio of error increases by selecting a bigger value for the order k. We also compared the obtained errors for the different numbers k and N in Fig. 4 drawn in the logarithmic mode. The error bound (22) justifies the results converge to the exact solution when $N\to\infty$ with the high order.

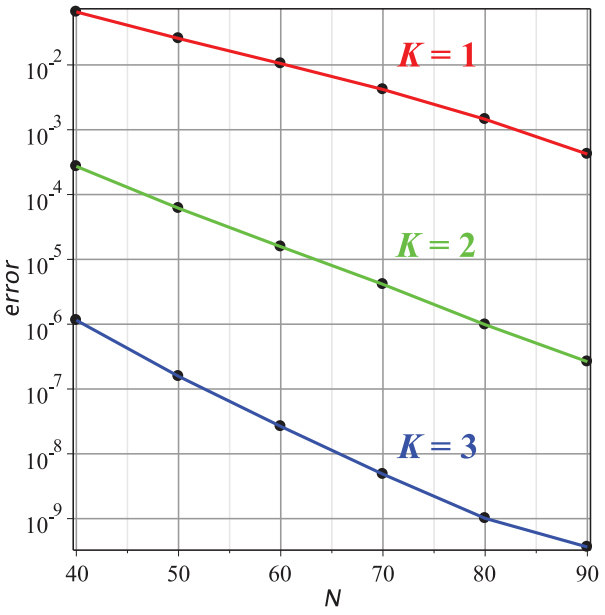

Fig. 5. Distribution of absolute error for Example 4.4.

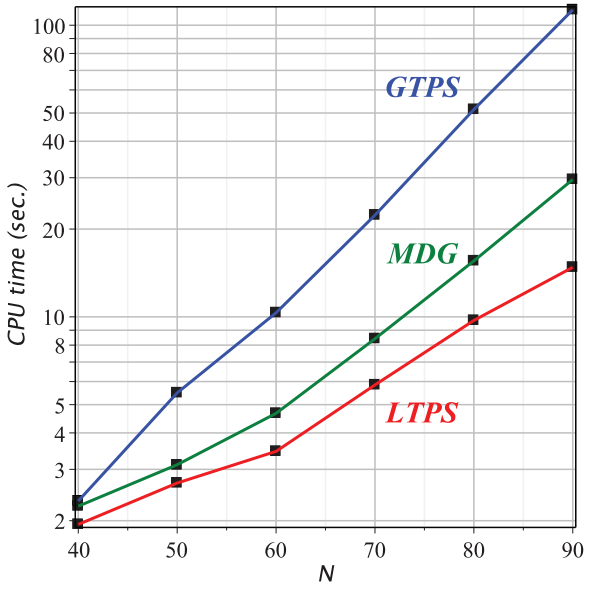

Fig. 6. CPU times for Example 4.4.

Example 4.4. Consider the following logarithmic integral equation:

$$u(t) - \frac{1}{\pi}\int_{-\pi}^{\pi}\left[\ln\left|2\sin\frac{t-s}{2}\right|\left\{\sinh\frac{t+s}{2}\,\sin^2\frac{t-s}{2}\right\} + \ln(t+10)\right]u(s)\mathrm{d}s = f(t) \tag{26}$$

where the function $f(t)$ has been so chosen that the exact solution is

$$u_{ex}(x) = \frac{te^t}{t^2+e}.$$

Table 4 reports $\|e\|_\infty$, $\|e\|_2$ and the values of the ratio at different numbers of N and k. We also solve the integral Eq. (26) utilizing the MDG method and the numerical results are given in Table 6. The obtained errors for different numbers of N are drawn in the logarithmic mode in Fig. 4. We have compared the CPU times (sec.) for solving this integral equation using global and local MDG and MDG approach for different numbers of N in Fig. 5. These results show the presented

Table 6
Some numerical results for Example 4.4 using the MDG method.

N	$q=1$			$q=2$		
	δ	$\|e_N\|_2$	$\|e_N\|_\infty$	δ	$\|e_N\|_2$	$\|e_N\|_\infty$
40	0.051	4.52e-03	8.49e-03	0.077	1.15e-04	2.16e-04
50	0.041	2.96e-03	5.44e-03	0.061	5.86e-05	1.12e-04
60	0.034	1.98e-03	3.79e-03	0.051	3.41e-05	6.52e-05
70	0.029	1.51e-03	2.76e-03	0.043	2.17e-05	4.16e-05
80	0.025	1.14e-03	2.11e-03	0.038	1.43e-05	2.78e-05
90	0.022	8.86e-04	1.65e-03	0.034	9.94e-06	1.93e-05

method in the current paper, in comparison with the method based on the globally supported RBFs and MDG for solving logarithmic integral equations, uses much less computer memory and times (Fig. 6).

5. Conclusion

This article has studied an efficient technique for numerically solving a class of Fredholm integral equations of the second kind with logarithmic-singular kernels. These types of integral equations result from boundary value problems of two-dimensional Helmholtz equations with the Robin boundary conditions. The method uses locally supported thin plate splines constructed on scattered points as a basis in the discrete collocation method. The singular integrals occurred in this method have been computed utilizing a composite non-uniform Gauss–Legendre integration rule. We have also investigated the error estimate of the new approach. The proposed scheme has been constructed on a set of scattered data and does not require any background meshes, so it is meshless. As demonstrated by the numerical results, the proposed technique is able to produce accurate solutions with the low CPU time for various types of logarithmic integral equations.

Acknowledgments

The authors are very grateful to the three reviewers for their valuable comments and suggestions which have improved the paper.

References

[1] H. Adibi, P. Assari, On the numerical solution of weakly singular Fredholm integral equations of the second kind using Legendre wavelets, J. Vib. Control 17 (2011) 689–698.
[2] P. Assari, H. Adibi, M. Dehghan, A meshless method for solving nonlinear two-dimensional integral equations of the second kind on non-rectangular domains using radial basis functions with error analysis, J. Comput. Appl. Math. 239 (2013) 72–92.
[3] P. Assari, H. Adibi, M. Dehghan, A meshless discrete Galerkin (MDG) method for the numerical solution of integral equations with logarithmic kernels, J. Comput. Appl. Math. 267 (2014) 160–181.
[4] P. Assari, H. Adibi, M. Dehghan, A meshless method based on the moving least squares (MLS) approximation for the numerical solution of two-dimensional nonlinear integral equations of the second kind on non-rectangular domains, Numer. Algorithms 67 (2014) 423–455.
[5] P. Assari, H. Adibi, M. Dehghan, The numerical solution of weakly singular integral equations based on the meshless product integration (MPI) method with error analysis, Appl. Numer. Math. 81 (2014) 76–93.
[6] P. Assari, M. Dehghan, The numerical solution of two-dimensional logarithmic integral equations on normal domains using radial basis functions with polynomial precision, Eng. Comput. 33 (2017) 853–870.
[7] P. Assari, M. Dehghan, Solving a class of nonlinear boundary integral equations based on the meshless local discrete Galerkin (MLDG) method, Appl. Numer. Math. 123 (2018) 137–158.
[8] K.E. Atkinson, The Numerical Solution of Integral Equations of the Second Kind, Cambridge University Press, Cambridge, 1997.
[9] I.M. Babuska, F. Ihlenburg, E.T. Paik, S.A. Sauter, A generalized finite element method for solving the Helmholtz equation in two dimensions with minimal pollution, Comput. Methods Appl. Mech. Eng. 128 (1995) 325–359.
[10] P. Baratella, A note on the convergence of product integration and Galerkin method for weakly singular integral equations, J. Comput. Appl. Math. 85 (1997) 11–18.
[11] A. Bejancu Jr, Local accuracy for radial basis function interpolation on finite uniform grids, J. Approx. Theory 99 (1999) 242–257.
[12] Y. Cao, M. Huang, L. Liu, Y. Xu, Hybrid collocation methods for Fredholm integral equations with weakly singular kernels, Appl. Numer. Math. 57 (2007) 549–561.
[13] R. Cavoretto, T. Schneider, P. Zulian, OpenCL based parallel algorithm for RBF-PUM interpolation, J. Sci. Comput. 74 (2018) 267–289.
[14] W. Chen, W. Lin, Galerkin trigonometric wavelet methods for the natural boundary integral equations, Appl. Math. Comput. 121 (2001) 75–92.
[15] A.C. Chrysakis, G. Tsamasphyros, Numerical solution of integral equations with a logarithmic kernel by the method of arbitrary collocation points, Int. J. Numer. Methods Eng. 33 (1992) 143–148.
[16] C.-H. Jo, C. Shin, J.H. Suh, An optimal 9-point, finite-difference, frequency-space, 2-d scalar wave extrapolator, Geophysics 61 (1996) 529–537.
[17] S. Cuomo, A. Galletti, G. Giunta, L. Marcellino, Reconstruction of implicit curves and surfaces via RBF interpolation, Appl. Numer. Math. 116 (2017) 157–171.
[18] S. Cuomo, A. Galletti, G. Giunta, A. Starace, Surface reconstruction from scattered point via RBF interpolation on GPU, in: Proceedings of the Federated Conference on Computer Science and Information Systems, 2013, pp. 433–440.
[19] M. Dehghan, M. Abbaszadeh, The meshless local collocation method for solving multi-dimensional Cahn-Hilliard, Swift-Hohenberg and phase field crystal equations, Eng. Anal. Bound. Elem. 78 (2017) 49–64.
[20] M. Dehghan, M. Abbaszadeh, The space-splitting idea combined with local radial basis function meshless approach to simulate conservation laws equations, Alexandria Eng. J. (2016), doi:10.1016/j.aej.2017.02.024.
[21] M. Dehghan, A. Nikpour, Numerical solution of the system of second-order boundary value problems using the local radial basis functions based differential quadrature collocation method, Appl. Math. Model. 37 (2013) 8578–8599.

[22] M. Dehghan, M. Nourian, M.B. Menhaj, Numerical solution of Helmholtz equation by the modified Hopfield finite difference techniques, Numer. Methods Partial. Differ. Equ. 25 (2009) 637–656.
[23] M. Dehghan, R. Salehi, The numerical solution of the non-linear integro-differential equations based on the meshless method, J. Comput. Appl. Math. 236 (2012) 2367–2377.
[24] V. Dominguez, High-order collocation and quadrature methods for some logarithmic kernel integral equations on open arcs, J. Comput. Appl. Math. 161 (2003) 145–159.
[25] W. Fang, Y. Wang, Y. Xu, An implementation of fast wavelet Galerkin methods for integral equations of the second kind, J. Sci. Comput. 20 (2004) 277–302.
[26] G.E. Fasshauer, Meshfree methods, in: Handbook of Theoretical and Computational Nanotechnology, American Scientific Publishers, 2005.
[27] W.Z. Feng, K. Yang, M. Cui, X.W. Gao, Analytically-integrated radial integration BEM for solving three-dimensional transient heat conduction problems, Int. Commun. Heat Mass Transf. 79 (2016) 21–30.
[28] Z. Fu, W. Chen, L. Ling, Method of approximate particular solutions for constant- and variable-order fractional diffusion models, Eng. Anal. Bound. Elem. 57 (2015) 37–46.
[29] Z. Fu, W. Chen, H. Yang, Boundary particle method for laplace transformed time fractional diffusion equations, J. Comput. Phys. 235 (2013) 52–66.
[30] X.W. Gao, C. Zhang, L. Guo, Boundary-only element solutions of 2d and 3d nonlinear and nonhomogeneous elastic problems, Eng. Anal. Bound. Elem. 31 (2007) 974–982.
[31] A. Golbabai, E. Mohebianfar, H. Rabiei, On the new variable shape parameter strategies for radial basis functions, Comput. Appl. Math. 34 (2015) 691–704.
[32] A.A. Gusenkova, N.B. Pleshchinskii, Integral equations with logarithmic singularities in the kernels of boundary-value problems of plane elasticity theory for regions with a defect, J. Appl. Math. Mech. 64 (2000) 435–441.
[33] J. Guo, J.H. Jung, Radial basis function ENO and WENO finite difference methods based on the optimization of shape parameters, J. Sci. Comput. 70 (2017) 551–575.
[34] J. Guo, J.H. Jung, A RBF-WENO finite volume method for hyperbolic conservation laws with the monotone polynomial interpolation method, Numer. Math. 122 (2017) 27–50.
[35] Y. Hon, B. Sarler, D. Yun, Local radial basis function collocation method for solving thermo-driven fluid-flow problems with free surface, Eng. Anal. Bound. Elem. 57 (2015) 2–8.
[36] H. Hosseinzadeh, M. Dehghan, A new scheme based on boundary elements method to solve linear Helmholtz and semi-linear Poisson's equations, Eng. Anal. Bound. Elem. 43 (2014) 124–135.
[37] H. Kaneko, Y. Xu, Gauss-type quadratures for weakly singular integrals and their application to Fredholm integral equations of the second kind, Math. Comput. 62 (1994) 739–753.
[38] S.A. Khuri, A.M. Wazwaz, The decomposition method for solving a second kind Fredholm integral equation with a logarithmic kernel, Int. J. Comput. Math. 61 (1996) 103–110.
[39] G. Kosec, B. Sarler, Solution of a low Prandtl number natural convection benchmark by a local meshless method, Int. J. Numer. Methods Heat Fluid Flow 23 (2013) 189–204.
[40] B. Kress, Linear Integral Equations, Springer-Verlag, Berlin, 1989.
[41] C.K. Lee, X. Liu, S.C. Fan, Local multiquadric approximation for solving boundary value problems, Comput. Mech. 30 (2003) 396–409.
[42] X. Li, Meshless Galerkin algorithms for boundary integral equations with moving least square approximations, Appl. Numer. Math. 61 (2011) 1237–1256.
[43] X. Li, J. Zhu, A Galerkin boundary node method and its convergence analysis, J. Comput. Appl. Math. 230 (2009) 314–328.
[44] X. Li, J. Zhu, A Galerkin boundary node method for Biharmonic problems, Eng. Anal. Bound. Elem. 33 (2009) 858–865.
[45] X. Li, J. Zhu, A meshless galerkin method for stokes problems using boundary integral equations, Comput. Methods Appl. Mech. Engrg. 198 (2009) 2874–2885.
[46] G. Long, G. Nelakanti, X. Zhang, Iterated fast multiscale Galerkin methods for Fredholm integral equations of second kind with weakly singular kernels, Appl. Numer. Math. 62 (2012) 201–211.
[47] B. Mavric, B. Sarler, Local radial basis function collocation method for linear thermoelasticity in two dimensions, Int. J. Numer. Methods Heat Fluid Flow 25 (2015) 1488–1510.
[48] J. Meinguet, Multivariate interpolation at arbitrary points made simple, Z. Angew. Math. Phys. 30 (1979) 292–304.
[49] D. Mirzaei, M. Dehghan, A meshless based method for solution of integral equations, Appl. Numer. Math. 60 (2010) 245–262.
[50] K. Mramor, R. Vertnik, B. Sarler, Simulation of natural convection influenced by magnetic field with explicit local radial basis function collocation method, CMES Comput. Model. Eng. Sci. 92 (2013) 327–352.
[51] F.J. Narcowich, N. Sivakumar, J.D. Ward, On condition numbers associated with radial-function interpolation, J. Math. Anal. Appl. 186 (1994) 457–485.
[52] T. Okayama, T. Matsuo, M. Sugihara, Sinc-collocation methods for weakly singular Fredholm integral equations of the second kind, J. Comput. Appl. Math. 234 (2010) 1211–1227.
[53] A. Pedas, G. Vainikko, Superconvergence of piecewise polynomial collocations for nonlinear weakly singular integral equations, J. Integral Equ. Appl. 9 (1997) 379–406.
[54] Y.V.S.S. Sanyasiraju, C. Satyanarayana, On optimization of the RBF shape parameter in a grid-free local scheme for convection dominated problems over non-uniform centers, Appl. Math. Model. 37 (2013) 7245–7272.
[55] S.A. Sarra, A local radial basis function method for advection-diffusion-reaction equations on complexly shaped domains, Appl. Math. Comput. 218 (2012) 9853–9865.
[56] M. Scheuerer, An alternative procedure for selecting a good value for the parameter C in RBF-interpolation, Adv. Comput. Math. 34 (2011) 105–126.
[57] C. Shu, H. Ding, K.S. Yeo, Local radial basis function-based differential quadrature method and its application to solve two-dimensional incompressible Navier–Stokes equations, Comput. Methods Appl. Mech. Eng. 192 (2003) 941–954.
[58] J. Sun, H. Yi, H. Tan, Local radial basis function meshless scheme for vector radiative transfer in participating media with randomly oriented axisymmetric particles, Appl. Opt. 55 (2016) 1232–1240.
[59] S.u. Islam, B. Sarler, R. Vertnik, G. Kosec, Radial basis function collocation method for the numerical solution of the two-dimensional transient nonlinear coupled burgers' equations, Appl. Math. Model. 36 (2012) 1148–1160.
[60] Siraj-Ul-Islam, R. Vertnik, B. Sarler, Local radial basis function collocation method along with explicit time stepping for hyperbolic partial differential equations, Appl. Numer. Math. 67 (2013) 136–151.
[61] E. Turkel, D. Gordon, R. Gordon, S. Tsynkov, Compact 2d and 3d sixth order schemes for the Helmholtz equation with variable wave number, J. Comput. Phys. 232 (2013) 272–287.
[62] R. Vertnik, B. Sarler, Local collocation approach for solving turbulent combined forced and natural convection problems, Adv. Appl. Math. Mech. 3 (2011) 259–279.
[63] R. Vertnik, B. Sarler, Meshless local radial basis function collocation method for convective-diffusive solid-liquid phase change problems, Int. J. Numer. Methods Heat Fluid Flow 16 (2006) 617–640.
[64] G. Wahba, Convergence rate of "thin plate" smoothing splines when the data are noisy (preliminary report), Springer Lecture Notes Math. 757 (1979) 233–245.
[65] B. Wang, A local meshless method based on moving least squares and local radial basis functions, Eng. Anal. Bound. Elem. 50 (2015) 395–401.
[66] A.M. Wazwaz, R. Rach, J. Duan, The modified Adomian decomposition method and the noise terms phenomenon for solving nonlinear weakly-singular volterra and fredholm integral equations, Cent. Eur. J. Eng. 3 (2013) 669–678.

[67] H. Wendland, Scattered Data Approximation, Cambridge University Press, New York, 2005.
[68] G. Yao, J. Duo, C.S. Chen, L.H. Shen, Implicit local radial basis function interpolations based on function values, Appl. Math. Comput. 265 (2015) 91–102.
[69] G. Yao, B. Sarler, C.S. Chen, A comparison of three explicit local meshless methods using radial basis functions, Eng. Anal. Bound. Elem. 35 (2011) 600–609.
[70] D.F. Yun, Y.C. Hon, Improved localized radial basis function collocation method for multi-dimensional convection-dominated problems, Eng. Anal. Bound. Elem. 67 (2016) 63–80.